

Design of Dry Dual Clutch Transmission Actuator Controller for Simultaneous Kissing Point Identification Using Multiple Sliding Surfaces

Jiwon Oh¹ and Seibum B. Choi²

¹ School of Mechanical Aerospace & Systems Engineering, Division of Mechanical Engineering,
 Korea Advanced Institute of Science and Technology, Daejeon, Korea
 (Tel : +82-42-350-4104; E-mail: jwo@kaist.ac.kr)

² School of Mechanical Aerospace & Systems Engineering, Division of Mechanical Engineering,
 Korea Advanced Institute of Science and Technology, Daejeon, Korea
 (Tel : +82-42-350-4120; E-mail: sbchoi@kaist.ac.kr)

Abstract: This paper suggests a dry dual clutch transmission actuator controller for simultaneous kissing point identification by using multiple sliding surfaces, so that the actuator motor positions at the clutch kissing point of both clutches can be estimated during the first launching after the car starts. Such maneuver can be especially advantageous for the vehicles without ROM that keeps the recent kissing point estimations. Separate multiple sliding surface controllers are designed for each actuator, and PI-type actuator motor model-based observers are designed to swiftly identify the kissing point position relative to the initial motor position measured by incremental encoders attached to each actuator motor. Also, methodologies to reduce the jerk that may arise from the simultaneous kissing point identification are suggested. The controller and estimation performance is verified by taking the entire driveline with the forward and reverse engine torque map, physical parameters of the transmission, and actuator model into consideration, and simulations are conducted with the inclusion of sensor measurement noise and friction model to reflect realistic vehicle driveline using MATLAB/Simulink.

Keywords: dual clutch transmission, clutch kissing point, multiple sliding surface, observer, powertrain.

Nomenclature

θ	shaft angle
k	spring constant
b	damping coefficient
J	moment of inertia
T	torque
ω	angular velocity
F_n	normal force
i_{t1}	T/M gear ratio for transfer shaft 1
i_{t2}	T/M gear ratio for transfer shaft 2
i_{f1}	final reduction gear ratio for transfer shaft 1
i_{f2}	final reduction gear ratio for transfer shaft 2
α_{th}	throttle angle
Subscript e	engine
Subscript d	external damper
Subscript $c1$	clutch 1 speed (input shaft 1)
Subscript $c2$	clutch 2 speed (input shaft 2)
Subscript $t1$	transfer shaft 1
Subscript $t2$	transfer shaft 2
Subscript o	output shaft
Subscript w	wheel
Subscript v	vehicle
Subscript m	motor
Subscript 1	actuator 1
Subscript 2	actuator 2
Subscript dia	diaphragm spring

clutch control algorithm has been considerably increasing. Most of the electromechanical clutch actuator controller algorithms already developed are based on the actuator position or clutch stroke to control the amount of torque transferred through the clutch. However, little attention is paid to the methods for kissing point estimation, which can significantly influence the launch or gear shift quality.

For the vehicles without ROM, since the initial actuator position is unknown when the car starts, the initialization procedure is required. For this, the actuator needs to retract backward, away from the clutch, to be able to assign absolute position to the relative position measured by the incremental encoder. However, such process takes time, and may be a source of inconvenience for impatient drivers.

Also, even if the absolute position can be provided through such initialization of the actuators, the absolute distance between the clutch plates is still not available, since the clutch friction disk surface position is unknown due to the degree of clutch wear. This information is crucial for the clutch actuator control, since controlling the clutch stroke without knowing at what position the clutch torque transfer begins – which is defined to be the clutch kissing point [1] – can lead to high amount of jerk and clutch life deterioration.

Since the majority of the conventional electromechanical clutch actuator controller makes use of the motor position for the application of feed-forward controller, such aforementioned background implies that performances obtained by previous works to control the automated manual transmission [2-5] and dual clutch transmission [6-10] especially during launching when

1. INTRODUCTION

With the proliferation of the dual clutch transmissions in production vehicles, the importance of the effective

the heat dissipation due to friction is maximal, can only be guaranteed with the provision of accurate kissing point information. However, most works overlook the importance of the kissing point estimation, and assume that it is already given [5, 10, 11].

Furthermore, the conventional kissing point identification procedure is two-fold, which can lead to degraded clutch control performance during the first launch and first gear shift. With the carefully designed launching controller, the kissing point of the first clutch of the dual clutch transmission can be identified while the vehicle launches at the cost of jerk in an acceptable range. However, the vehicle must then undergo another phase of degraded clutch control performance due to the absence of kissing point information for the second clutch, and this happens during the first gear shift when the first gear shifts up to the second gear.

Hence, to prevent such issue, this paper suggests the novel scheme of simultaneous control of both clutches during the launch, so that by the first gear shift, the kissing point positions for both clutches can be readily utilized for the position-based controller.

The rest of the paper is structured as follows. Section 2 briefly describes the system and the driveline model developed for the simulation. Section 3 deals with the model reference PI observer which identifies the kissing point. Section 4 focuses on the controller design for the separate actuators which enable the simultaneous kissing point estimation. Section 4 displays the results of the validation conducted to show the controller states and inputs related to the first launching which does not make use of the kissing point information, and also shows the estimated kissing points against the actual values.

2. SYSTEM DESCRIPTION

2.1 Driveline

The driveline model with dual transfer shaft compliance is used for simulation, whose structure is shown in fig. 1.

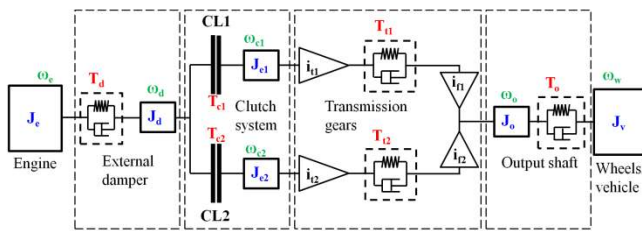


Fig. 1 Dual clutch transmission driveline model (J: inertia, T: torque, ω : angular velocity)

The dynamics of each part starting from the engine to the vehicle can be indicated in order as follows:

$$J_e \dot{\omega}_e = T_e - T_d \quad (1)$$

$$J_d \dot{\omega}_d = T_d - T_{c1} - T_{c2} \quad (2)$$

$$J_{e1} \dot{\omega}_{c1} = T_{c1} - \frac{T_{t1}}{i_{t1}} \quad (3)$$

$$J_{e2} \dot{\omega}_{c2} = T_{c2} - \frac{T_{t2}}{i_{t2}} \quad (4)$$

$$J_o \dot{\omega}_o = i_{f1} T_{t1} + i_{f2} T_{t2} - T_o \quad (5)$$

$$J_v \dot{\omega}_w = T_o i_f - T_v \quad (6)$$

The above dynamics stated from (1) to (7) correspond to the engine, external damper, clutches, output shaft, and wheel dynamics, respectively.

For each dynamics, the related torque is modeled as shown next.

$$T_e = f(\alpha_{th}, \omega_e) \quad (7)$$

Here, the net engine torque is defined as a function of throttle input and engine speed as a map. The external damper torque can be obtained using the known torsional spring and damping constants of the damper.

$$T_d = k_d (\theta_e - \theta_d) + b_d (\omega_e - \omega_d) \quad (8)$$

The clutch torque must be defined differently according to their phases as shown next.

$$T_{c1} = \begin{cases} 0 & , \text{ when disengaged} \\ \mu C_{c1} F_{n1} \text{sgn}(\omega_d - \omega_{c1}) & , \text{ when slipping} \\ \frac{T_{t1}}{i_{t1}} + J_{e1} \dot{\omega}_{c1} & , \text{ when engaged} \end{cases} \quad (9)$$

$$T_{c2} = \begin{cases} 0 & , \text{ when disengaged} \\ \mu C_{c2} F_{n2} \text{sgn}(\omega_d - \omega_{c2}) & , \text{ when slipping} \\ \frac{T_{t2}}{i_{t2}} + J_{e2} \dot{\omega}_{c2} & , \text{ when engaged} \end{cases} \quad (10)$$

Similar to (8), the transfer shaft and output shaft torques are defined using the shaft compliance model.

$$T_{t1} = k_{t1} \left(\frac{\theta_{c1}}{i_{t1}} - i_{f1} \theta_o \right) + b_{t1} \left(\frac{\omega_{c1}}{i_{t1}} - i_{f1} \omega_o \right) \quad (11)$$

$$T_{t2} = k_{t2} \left(\frac{\theta_{c2}}{i_{t2}} - i_{f2} \theta_o \right) + b_{t2} \left(\frac{\omega_{c2}}{i_{t2}} - i_{f2} \omega_o \right) \quad (12)$$

$$T_o = k_o (\theta_o - \theta_w) + b_o (\omega_o - \omega_w) \quad (13)$$

$$T_v = r_w \left(\underbrace{m_v g \sin(\theta_{road})}_{\text{road gradient}} + \underbrace{K_r m_v g \cos(\theta_{road})}_{\text{rolling resistance}} + \underbrace{\frac{1}{2} \rho v_x^2 C_d A}_{\text{aerodynamic drag}} \right) \quad (14)$$

2.2 Actuator

The actuator used for the simulation is operated with the ball screw driven by a motor, which is able to push the lever which is connected to the thrust bearing. The thrust bearing then pushes against the clutch disk and the diaphragm spring which provides normal force onto the friction disk surface. The simplified model of the actuator is shown in fig. 2.

Here, the lever angle θ_l is assumed negligible, and the clutch is designed to be normally open. The spring constant of the coupling, ball screw, and lever are combined together to give the equivalent spring

constant k_e . Also, the ball screw ratio, which is the quotient of θ_m and x_s is combined with the lever gain, a function of l_1 and l_2 , to give the equivalent ratio N .

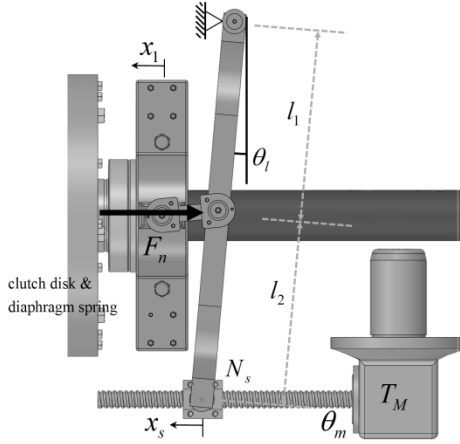


Fig. 2 Simplified diagram of the clutch actuator

Let us now focus on the side of the first clutch, CL1. the subscripts 1 and 2 henceforth denote the variables of CL1 side and those of CL2 side, respectively.

The following simplified driveline dynamics can be used for the model-based controller to be designed.

$$J_{e1}\dot{\omega}_{c1} = T_{c1} - \frac{T_o}{i_{11}i_{f1}} \quad (15)$$

Since the clutch torque is a function of normal reaction force and friction coefficient, it can be expressed as follows.

$$T_{c1} = F_{n1}C_{c1}\mu \operatorname{sgn}(\omega_d - \omega_{c1}) \quad (16)$$

where

$$F_{n1} = \begin{cases} k_{dial}(x_1 - x_{k1}), & x_1 \geq x_{k1} \\ 0, & \text{otherwise} \end{cases} \quad (17)$$

Now, by making use of the equivalent actuator spring constant and equivalent actuation ratio, the following expression for clutch stroke is obtained.

$$x_1 = \frac{1}{N_1} \left(\frac{T_{m1}}{k_{e1}} + \theta_{m1} \right) \quad (18)$$

The mechanical part of the motor dynamics is given next.

$$J_{m1}\ddot{\theta}_{m1} = T_{m1} - T_{fm1} - \frac{F_{n1}}{N_1} \quad (19)$$

where

$$T_{m1} = k_t i_1 \quad (20)$$

The friction torque T_{fm1} is modeled using LuGre friction model and the static Stribeck effect model. Further details can be found in [3]. The electrical dynamic model of the motor is shown as the following.

$$u_1 = R_m i_1 + L_m \frac{di_1}{dt} + V_{emf} \quad (21)$$

where

$$V_{emf} = k_m \dot{\theta}_{m1} \quad (22)$$

After substitution of (16) to (18) into (15), and likewise for the motor equations, the following dynamic equations for the actuator can be obtained.

$$J_{e1}\dot{\omega}_{c1} = \frac{k_{dial}C_{c1}\mu}{N_1 k_{e1}} k_t i_1 + \frac{k_{dial}C_{c1}\mu}{N_1} \theta_{m1} - k_{dial}C_{c1}\mu x_{k1} - \frac{T_o}{i_{11}i_{f1}} \quad (23)$$

$$J_{m1}\ddot{\theta}_{m1} = k_t i_1 - T_{fm1} - \frac{F_{n1}}{N_1} \quad (24)$$

$$u_1 = R_m i_1 + L_m \dot{i}_1 + k_m \dot{\theta}_{m1} \quad (25)$$

3. CLUTCH KISSING POINT IDENTIFICATION

For the clutch kissing point identification, a simple PI-type observer is developed based on the motor dynamics. Since the PI-observer first requires the model of the actuator without any load torque, equation (19) simplifies to the following.

$$J_{m1}\ddot{\theta}_{m1} = k_t i_1 - T_{fm1} \quad (26)$$

Based on this, the PI-type observer can be designed in shown next, where the “hat” on variables indicate estimation.

$$J_{m1}\dot{\hat{\omega}}_{m1} = k_t \hat{i}_1 - T_{fm1} + L_p (\omega_{m1} - \hat{\omega}_{m1}) + L_i \int (\omega_{m1} - \hat{\omega}_{m1}) dt \quad (27)$$

$$L_m \dot{\hat{i}}_1 = -k_m \hat{\omega}_{m1} - R_m \hat{i}_1 + u_1 \quad (28)$$

With zero or low correction feedback gains shown in (27), the observer may give acceptable estimation of the motor speed during the clutch disengaged phase. However, since the modeling of the clutch normal force, and thus the load torque, is omitted, the observer must depend on the feedback terms in order to give the accurate motor speed estimation. This inevitably leads to the sudden increase in the magnitude of the feedback term when the clutch begins to engage at the kissing point, and the kissing point can be easily found by using this phenomenon. In other words, the estimator logic takes the motor position value at the moment the feedback term exceeds a given threshold as the kissing point. Here, the threshold value must be carefully selected so that the algorithm does not mistakenly respond to noise.

The PI-observer for the CL2 can be designed in the similar manner. However, to reduce the amount of jerk that can be produced by simultaneous kissing of the two clutches, CL2 control for kissing point identification is delayed intentionally.

4. CONTROLLER DESIGN

4.1 Multiple-Surface Sliding Mode Controller

The sliding mode controller is chosen as the controller type, since it provides high tracking ability as far as the actuator bandwidth allows, and effectively

cancels the modeled disturbances that are extraneous to the desired state tracking control. Hence this type of controller is considered apt for the clutch stroke control without knowing the kissing point, since the kissing point must be found as quickly as possible and the clutch actuator must be able to suddenly retract in case of CL2.

4.1.1 Controller Design for Clutch 1

For the design of clutch 1 actuator controller, the CL1 dynamics obtained in (23) is used with the electrical dynamic model of the motor stated in (25).

First the sliding surface is defined as the discrepancy between the clutch speed and desired value, as shown next.

$$\lambda_{11} = \omega_{c1} - \omega_{c1d} \quad (29)$$

By differentiation of (29) and substituting (23) gives the following.

$$\begin{aligned} \dot{\lambda}_{11} &= \dot{\omega}_{c1} - \dot{\omega}_{c1d} \\ &= \frac{k_{dia1}k_t C_{c1}\mu}{J_{e1}N_1k_{e1}} \dot{i}_1 + \frac{k_{dia1}C_{c1}\mu}{J_{e1}N_1} \dot{\theta}_{m1} \\ &\quad - \frac{k_{dia1}C_{c1}\mu x_{k1}}{J_{e1}} - \frac{T_o}{J_{e1}i_{f1}} - \dot{\omega}_{c1d} \end{aligned} \quad (30)$$

$$\text{Let } \dot{\lambda}_{11}\lambda_{11} = -\eta\lambda_{11} \text{sgn}(\lambda_{11}) \rightarrow \dot{\lambda}_{11} = -\eta \text{sgn}(\lambda_{11}) \quad (31)$$

Then we obtain,

$$\frac{k_{dia1}k_t C_{c1}\mu}{J_{e1}N_1k_{e1}} \dot{i}_1 + \frac{k_{dia1}C_{c1}\mu}{J_{e1}N_1} \dot{\theta}_{m1} - \frac{k_{dia1}C_{c1}\mu x_{k1}}{J_{e1}} - \frac{T_o}{J_{e1}i_{f1}} \quad (32)$$

$$\equiv \dot{\omega}_{c1d} - K_{11} \text{sgn}(\lambda_{11})$$

From (32), the following desired current can be obtained.

$$\begin{aligned} i_{1d} &= -\frac{k_{e1}}{k_t} \dot{\theta}_{m1} + \frac{N_1k_{e1}x_{k1}}{k_t} + \frac{N_1k_{e1}T_o}{i_{f1}i_{f1}k_t k_{dia1}C_{c1}\mu} \\ &\quad + \frac{J_{e1}N_1k_{e1}}{k_t k_{dia1}C_{c1}\mu} \dot{\omega}_{c1d} - \frac{J_{e1}N_1k_{e1}K_{11}}{k_t k_{dia1}C_{c1}\mu} \text{sgn}(\lambda_{11}) \end{aligned} \quad (33)$$

The second sliding surface is defined as the following.

$$\lambda_{12} = i_1 - i_{1d} \quad (34)$$

With the similar steps exhibited for the first sliding surface, the following equations can be obtained.

$$\dot{\lambda}_{12} = \dot{i}_1 - \dot{i}_{1d} = -\frac{R_m}{L_m} i_1 - \frac{k_m}{L_m} \dot{\theta}_{m1} + \frac{1}{L_m} u_1 - \dot{i}_{1d} \quad (35)$$

$$L_m \dot{\lambda}_{12} = -R_m i_1 - k_m \dot{\theta}_{m1} + u_1 - L_m \dot{i}_{1d} \quad (36)$$

$$\text{Let } \dot{\lambda}_{12}\lambda_{12} = -\eta\lambda_{12} \text{sgn}(\lambda_{12}) \rightarrow \dot{\lambda}_{12} = -\eta \text{sgn}(\lambda_{12}) \quad (37)$$

$$u_1 \equiv R_m \hat{i}_1 + k_m \dot{\theta}_{m1} + L_m \dot{i}_{1d} - K_{12} \text{sgn}(\lambda_{12}) \quad (38)$$

Finally, the control input is calculated in (38). Notice how the current information is required to obtain the control input. It is replaced by the current estimation obtained by the motor current observer which is explained in section 4.2.

Beyond the identified kissing point for CL1, the controller may further be modified or replaced by another controller which now can utilize the estimated kissing point information for improved performance.

4.1.2. Controller Design for Clutch 2

The Controller for CL2 must be separately designed from that of CL1, since CL1 must proceed to launching control after the kissing point has been identified, whereas CL2 must retract back immediately after the kissing point has been found in order to reduce jerk and prevent backward torque recirculation problem which may take place within the internal structure of the transmission.

Until the identification of the CL2 kissing point, a controller that is similar to that for CL1 can be used, as shown next.

$$\begin{aligned} i_{2d} &= -\frac{k_{e2}}{k_t} \dot{\theta}_{m2} + \frac{N_2k_{e2}x_{k2}}{k_t} + \frac{N_2k_{e2}T_o}{i_{f2}i_{f2}k_t k_{dia2}C_{c2}\mu} \\ &\quad + \frac{J_{e2}N_2k_{e2}}{k_t k_{dia2}C_{c2}\mu} \dot{\omega}_{c2d} - \frac{J_{e2}N_2k_{e2}K_{21}}{k_t k_{dia2}C_{c2}\mu} \text{sgn}(\lambda_{21}) \end{aligned} \quad (39)$$

$$u_2 \equiv R_m \hat{i}_2 + k_m \dot{\theta}_{m2} + L_m \dot{i}_{2d} - K_{22} \text{sgn}(\lambda_{22}) \quad (40)$$

When the CL2 kissing point is found, the desired current is replaced by the following controller to quickly retract CL2.

First, the motor position tracking error is defined.

$$s_2 \equiv \theta_{m2} - \theta_{m2d} \quad (41)$$

Now sliding surface is designed and the motor dynamic model defined in (24) which corresponds to the CL2 is substituted as follows.

$$\begin{aligned} \dot{\lambda}_{23} &= \dot{s}_2 + \alpha s_2 = \ddot{\theta}_{m2} - \ddot{\theta}_{m2d} + \dot{\theta}_{m2} - \dot{\theta}_{m2d} \\ &= \frac{k_t}{J_{m2}} i_2 - \frac{T_{fm2}}{J_{m2}} - \frac{F_{n2}}{J_{m2}N_2} - \ddot{\theta}_{m2d} + \dot{\theta}_{m2} - \dot{\theta}_{m2d} \end{aligned} \quad (42)$$

$$\text{Let } \dot{\lambda}_{23}\lambda_{23} = -\eta\lambda_{23} \text{sgn}(\lambda_{23}) \rightarrow \dot{\lambda}_{23} = -\eta \text{sgn}(\lambda_{23}) \quad (43)$$

Then we obtain,

$$\begin{aligned} \frac{k_t}{J_{m2}} i_2 - \frac{T_{fm2}}{J_{m2}} - \frac{F_{n2}}{J_{m2}N_2} + \dot{\theta}_{m2} - \dot{\theta}_{m2d} \\ \equiv \ddot{\theta}_{m2d} - K_{23} \text{sgn}(\lambda_{23}) \end{aligned} \quad (44)$$

By isolating the current variable, the alternative desired current is computed as shown next.

$$\begin{aligned} i_{2d} &= \frac{T_{fm2}}{k_t} + \frac{F_{n2}}{N_2k_t} - \frac{J_{m2}}{k_t} \dot{\theta}_{m2} \\ &\quad + \frac{J_{m2}}{k_t} \dot{\theta}_{m2d} + \frac{J_{m2}}{k_t} \ddot{\theta}_{m2d} - \frac{J_{m2}K_{23}}{k_t} \text{sgn}(\lambda_{23}) \end{aligned} \quad (45)$$

The desired current obtained in (45) replaces that obtained in (39) when the kissing point for CL2 is identified.

4.2 Motor Current Estimation

By observing equation (38) and (40), it can be noticed that the computation of the control input requires the motor current information. Since the direct measurement of the motor current is not available, it must be estimated using an observer.

Here, an unknown input observer in proposed to

estimate the current based on the mechanical dynamic model of the motor. Recall (24). By isolating the motor acceleration, the following is reached.

$$\dot{\omega}_{m1} = \frac{k_t}{J_{m1}} \hat{i}_1 - \frac{T_{fm1}}{J_{m1}} - \frac{F_{n1}}{J_{m1}N_1} \quad (46)$$

Now, by considering the current as an unknown input, the following observer can be designed.

$$\dot{\hat{\omega}}_{m1} = \frac{k_t}{J_{m1}} \hat{i}_1 - \frac{T_{fm1}}{J_{m1}} - \frac{F_{n1}}{J_{m1}N_1} + l_{11}(\omega_{m1} - \hat{\omega}_{m1}) \quad (47)$$

$$\dot{\hat{i}}_1 = l_{12}(\omega_{m1} - \hat{\omega}_{m1}) \quad (48)$$

The current observer for CL2 is designed in the similar manner as well.

5. SIMULATION RESULT

The simulation is conducted to show the designed controller performance, current estimation accuracy, and clutch kissing point identification ability in an integrated manner. In all cases, the engine remains at the idle RPM for 1 second. Then the driver attempts to launch the vehicle by the ramp input, increasing the throttle to 20% during the next second, and the throttle input remains at 20% from then on. Integration with the active engine torque control to improve the launching quality shall be included in the future works.

Here, sensor measurement noise and friction model are deliberately included to maintain the simulation as realistic as possible.

Shown in fig. 3 is the current estimation result obtained by the unknown input observer discussed in section 4.2. The errors in the current estimation that can be seen between 1-1.5 seconds are caused by the incomplete kissing point estimation. Since the unknown input observer requires the normal force information which is largely influenced by the kissing point as indicated in (17), its estimation accuracy can temporarily be degraded, but converges back to the actual value immediately after the kissing point is identified.

As discussed before, the kissing point identification utilizes the phenomenon in which the correction feedback term increases to correct the PI-type observer estimation value as the effect of clutch engagement begins to disturb the system. This correction feedback term is plotted and shown with the PI-type observer estimated motor position and measured motor position in fig. 4. It can be indeed seen that the feedback term abruptly increases at the moment the motor position pushes beyond the kissing point, for both cases of actuator 1 and 2.

It can be also checked in fig. 4 (b) that the motor 2 controller effectively retracts the clutch back to 0, since the desired motor position is set to 0 at the cue of kissing point identification completion.

Fig. 5 shows the kissing point estimation accuracy. When the estimated kissing points are compared against the actual values, they almost coincide exactly when the identification is completed. The steady state error is shown to be less than 5%.

The states related to clutch control for simultaneous kissing point identification during launching are shown in fig. 6 to fig. 8, where fig 6 displays the control input voltage for each motor, fig. 7 shows the clutch torques transferred through each clutch with other driveline

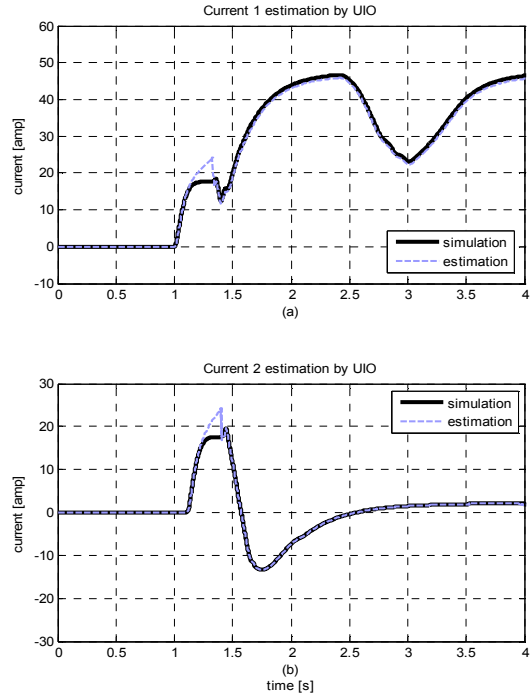


Fig. 3 Motor current estimation result by the unknown input observer. (a): current estimation of motor for CL1, (b): current estimation of motor for CL2

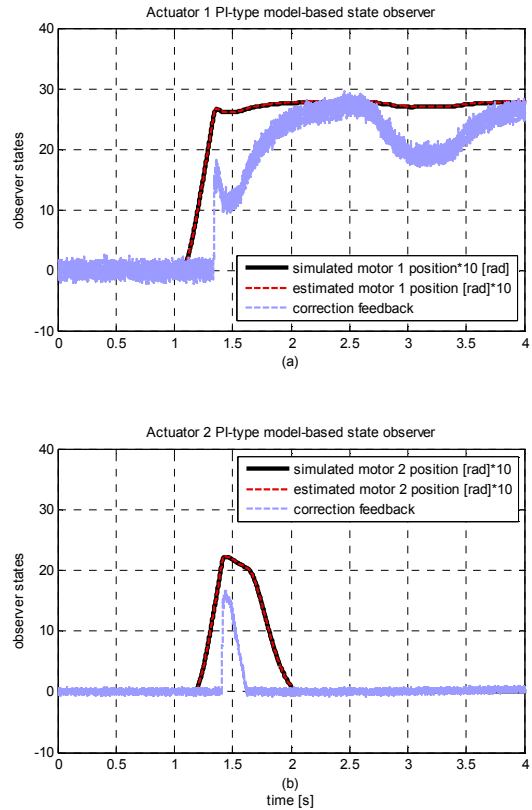


Fig. 4 Motor position estimation by PI-type observer and correction feedback magnitude for (a) CL1 actuator and (b) CL2 actuator

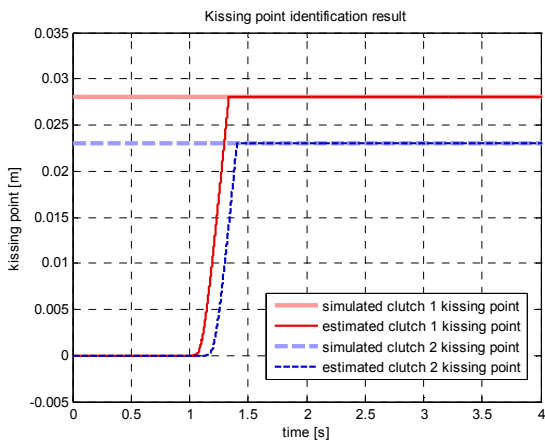


Fig. 5 Kissing point estimation result for CL1 and CL2

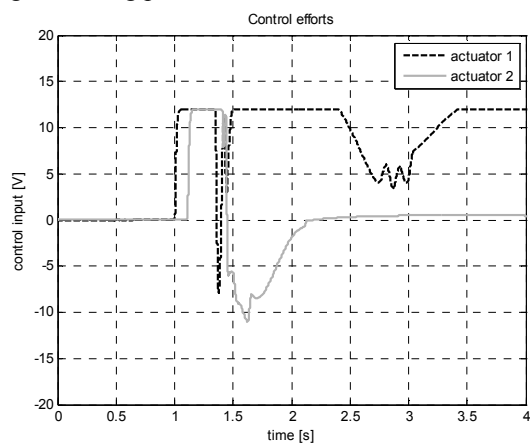


Fig. 6 Plot of control input for motors on CL1 and CL2

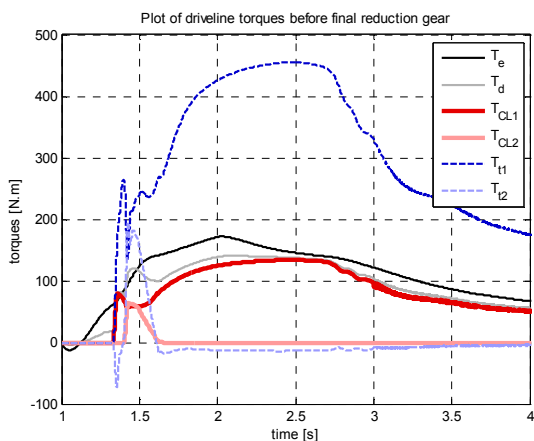


Fig. 7 Torques obtained by launching simulation during the simultaneous kissing point identification process

torques, and fig. 8 shows the angular velocities of the driveline. Although some jerk exists at the beginning of the launching process due to unknown kissing point, the sliding mode controller effectively manages to smoothly regulate the clutch slip to zero from then on, as shown in fig. 8. Fig. 9 displays the same angular velocities as those in fig. 8, but they are recorded during the single kissing point identification where only the estimation of the CL1 kissing point is conducted. No significant increase in jerk can be found in the comparison of the

two cases, which implies that the simultaneous identification of the kissing point by operating two clutch actuators during launch is possible with acceptable jerk.

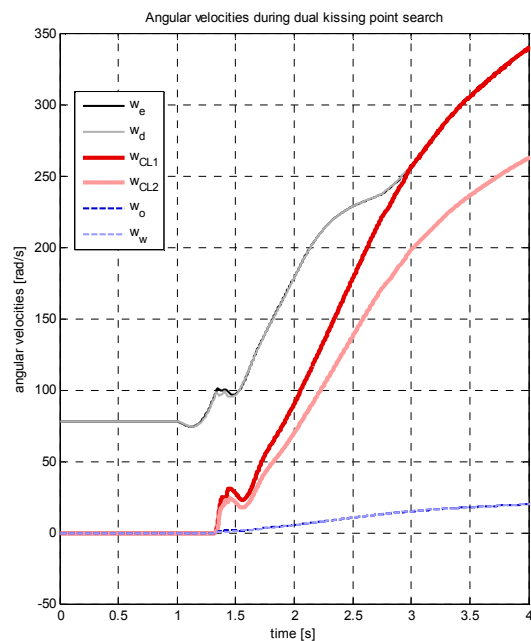


Fig. 8 Plot of angular velocities during the simultaneous kissing point identification process

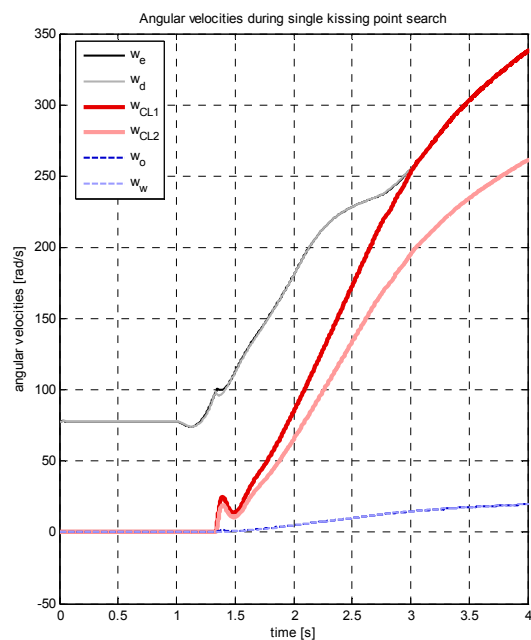


Fig. 9 Plot of angular velocities during the single kissing point identification process

5. CONCLUSION

This study has proposed novel method to effectively identify the kissing point of both clutches of the dual clutch transmissions. Making use of only the available

set of data in the transmission controller of current production vehicles, the proposed algorithm controls two clutch actuators simultaneously to estimate the clutch kissing point while the vehicle launches, so that the kissing point of the second clutch can be readily used for the first gear shift control. Summarizing the paper, two noteworthy contributions of the work are the following: ability for rapid and accurate engagement and disengagement of the clutches enabled by the multiple surface sliding mode controller, and development of a method to estimate the clutch kissing points of two clutches before launching ends. The work shall be further extended to develop clutch control algorithms that can be applied immediately after the kissing point information is ready, to give smoother control performance by directly making use of the identified kissing points.

ACKNOWLEDGEMENT

This work was supported by the National Research Foundation of Korea (NRF) grant funded by the Korea government (MSIP) (No. 2010-0028680), Global Ph. D. Fellowship Program, and C-ITRC (Convergence Information Technology Research Center) support program (NIPA-2013-H0401-13-1008) supervised by the NIPA (National IT Industry Promotion Agency).

REFERENCES

- [1] M. Song, J. Oh, H. Kim, "Engine clutch control algorithm during mode change for parallel hybrid electric vehicle," *Vehicle Power and Propulsion Conference (VPPC), 2012 IEEE*, pp.1118-1121, 9-12 Oct. 2012.
- [2] J. Horn, J. Bamberger, P. Michau, and S. Pindl, "Flatness-based clutch control for automated manual transmissions," *Control Eng. Pract.*, vol. 11, no. 12, pp. 1353–1359, 2003.
- [3] J. Kim, J. Oh, S. B. Choi, "Nonlinear Estimation Method of a Self-Energizing Clutch Actuator Load," *International Conference on Innovative Engineering Systems*, Alexandria, Egypt, Dec. 2012.
- [4] J. Kim and S. B. Choi, "Control of dry clutch engagement for vehicle launches via a shaft torque observer," *American Control Conference (ACC)*, pp. 676-681, 2010.
- [5] J. Deur, V. Ivanović, Z. Herold, M. Kostelac, and H. E. Tseng, "Dry clutch control based on electromechanical actuator position feedback loop," *International Journal of Vehicle Design*, vol. 60, no. 3, pp. 305-326, 2012.
- [6] X. Yao, D. Qin, and Z. Liu, "Simulation and Analysis of the Dual-Clutch Transmission Starting Control," *Journal of Chongqing university (natural science edition)*, vol. 1, no. 003, 2007.
- [7] M. X. Wu, J. W. Zhang, T. L. Lu, and C. S. Ni, "Research on optimal control for dry dual-clutch engagement during launch," *Proceedings of the Institution of Mechanical Engineers, Part D: Journal of Automobile Engineering*, vol. 224, no. 6, pp. 749-763, 2010.
- [8] V. N. Tran, J. Lauber, and M. Dambrine, "Sliding mode control of a dual clutch during launch," *The Second International Conference on Engineering Mechanics and Automation (ICEMA2)*, Hanoi, August 16-17, 2012.
- [9] J. Kim, S. B. Choi, H. Lee, J. Kang, and M. Hur, "System Modeling and Control of a Clutch Actuator System for Dual Clutch Transmissions," *KSAE Annual Conference & Exhibition*, pp. 1253-1257, 2011.
- [10] J. Kim, S. B. Choi, H. Lee, J. Koh, "Design of a Robust Internal-loop Compensator of Clutch Positioning Systems," *Proceedings of IEEE Multi-Conference on Systems and Control 2012*, Dubrovnik, Croatia.
- [11] J. Kim and S. B. Choi, "Self-energizing Clutch Actuator System: Basic Concept and Design," *Proceedings of FISITA 2010 World Automotive Congress*, Budapest, Hungary, 2010.